Research Article

Expansions and contractions of the inverted repeat, as well as gene loss and potential pseudogenization shape plastome evolution in Hechtioideae (Bromeliaceae, Poales)

Iván M. Ramírez-Morillo[1] , Laura A. Espinosa-Barrera[1,2]*, Carolina Granados Mendoza[3], Sandra I. Vera-Paz[3,4], Daniel D. Díaz Contreras Díaz[3,4], and Katya J. Romero-Soler[1,3]*

[1]Unidad de Recursos Naturales, Centro de Investigación Científica de Yucatán A. C., Mérida 97205, Yucatán, Mexico
[2]Laboratorio de Agrobiotecnología, Tecnoparque CLQ, Universidad de Colima, Colima 28629, Mexico
[3]Departamento de Botánica, Instituto de Biología, Universidad Nacional Autónoma de México, Coyoacán, Mexico City 04510, Mexico
[4]Posgrado en Ciencias Biológicas, Universidad Nacional Autónoma de México, Coyoacán, Mexico City 04510, Mexico
*Authors for correspondence. Katya J. Romero-Soler. E-mail: katya.romero@st.ib.unam.mx/katya.soler@gmail.com; Laura A. Espinosa-Barrera. E-mail: lauespinosaba@gmail.com

Abstract Full plastomes have recently proven to be a valuable data source for resolving recalcitrant phylogenetic relationships in the flowering plant family Bromeliaceae. The study of complete plastomes has additionally led to the discovery of new structural rearrangements and advanced our understanding of bromeliad plastome diversity and evolution. Here, we focus on the study of full plastomes of the bromeliad subfamily Hechtioideae to assess phylogenetic relationships, marker informativeness, and plastome structure and evolution. Using whole-genome sequencing data, we *de novo* assembled and annotated new plastid genomes of 19 Hechtioideae species plus one representative each from the Pitcairnioideae and Puyoideae subfamilies and compared them with four additional available plastomes from other bromeliad subfamilies. Our phylogenetic analysis using complete plastome sequences not only recovered the three currently recognized genera of Hechtioideae as monophyletic, strongly supporting *Mesoamerantha* as sister of *Bakerantha* and *Hechtia*, but also improved statistical support at different phylogenetic depths within the subfamily. We identified a set of highly informative loci, some of them explored for the first time in Hechtioideae. Structural rearrangements, including expansions and contractions of the inverted repeats, large inversions, and gene loss and potential pseudogenization were detected mainly within the genus *Hechtia*. Evolutionary trait rate shifts were associated with the size and guanine–cytosine content of the small single copy and inverted repeats.

Key words: Bromeliaceae, Hechtioideae, *ndh* gene family, phylogenetic informativeness, phylogenomics, plastid genome, structural rearrangements.

1 Introduction

Hechtioideae is one of the eight subfamilies currently recognized for Bromeliaceae (Givnish et al., 2007), comprising nearly 93 rupicolous and terrestrial species (Gouda et al., 2023), which are conspicuous elements of xeric shrublands and deciduous tropical forests of the Neotropics (Ramírez-Morillo et al., 2018a; Rivera-Martínez et al., 2022). Although distributed from southern United States to northern Nicaragua, Hechtioideae species diversity is centered in Mexico, where a recent phylogenetic analysis proposed that this lineage experienced high speciation rates during the last 6.5–1 million years ago (Mya; Rivera-Martínez et al., 2022). This subfamily is defined by a combination of morphological characteristics, including rosettes with

succulent leaves and spiny or rarely entire margins, dioecy, central or lateral inflorescences, unisexual and fragrant flowers, capsular fruits with winged to almost naked seeds, and the absence of stellate chlorenchyma (Givnish et al., 2007; Ramírez-Morillo et al., 2018a).

The phylogenetic relationships in Hechtioideae have previously been based on a few plastid (*rpl32-trnL* IGS, *rps16-trnK* IGS, *matK* gene, and *ycf1* gene) and one nuclear (*PRK* gene) loci, used to address different taxonomic scales (Ramírez-Morillo et al., 2018a; Rivera-Martínez et al., 2022; Romero-Soler et al., 2022a, 2022b). These studies have contributed evidence for the recognition of three genera: *Bakerantha* L.B. Sm. (five spp.), *Mesoamerantha* I. Ramírez & K. Romero (three spp.), and *Hechtia* Klotzsch *s. str.* (85 spp.). However, highly supported (bootstrap support (BS) > 85)

discordant phylogenetic relationships have been retrieved among these three genera when analyzing data from different genome compartments. In Ramírez-Morillo et al. (2018a), where the first phylogenetic hypothesis of the subfamily was proposed, an analysis of the *rpl32-trnL* and *ycf1* plastid markers retrieved *Bakerantha* (therein identified as clade B) as a sister of a clade including *Mesoamerantha* (therein identified as clade C) and *Hechtia*, whereas the analysis of the *PRK* nuclear gene by the same authors found a clade including *Mesoamerantha* and *Bakerantha* as the sister of *Hechtia*. Within the large genus *Hechtia*, three main clades, named clades D, E, and F, have been recovered with strong statistical support; however, the relationships among them remain uncertain due to a lack of resolution and statistical support (Ramírez-Morillo et al., 2018a; Rivera-Martínez et al., 2022). The clade D of *Hechtia* has the widest geographical distribution in the subfamily and corresponds to the *H. glomerata* Zuccharini species complex, which includes species with lateral inflorescences densely covered by a white-lepidote indument and white petals, except *H. pretiosa* Espejo & López-Ferrari, which has pink petals. The clade E of *Hechtia* includes the only two species in the subfamily with a completely inferior ovary, namely, *H. deceptrix* I. Ramírez & C. T. Hornung and *H. epigyna* Harms from northeastern Mexico, while the clade F of *Hechtia*, which includes about 84% of *Hechtia* species incorporated so far in phylogenetic reconstructions (Rivera-Martínez et al., 2022), is composed of several morphologically diverse and geographically restricted lineages, within which species-level relationships lack resolution and statistical support. The difficulty in obtaining resolved and highly supported phylogenetic hypotheses in Hechtioideae, as well as in other Bromeliaceae lineages (e.g., Puyoideae; Jabaily & Sytsma, 2010; core Bromelioideae, Sass & Specht, 2010), has been attributed to the low sequence variation resulting from low substitution rates in Bromeliaceae compared to other Commelinids groups (Smith & Donoghue, 2008; Palma-Silva et al., 2016).

Next-generation sequencing (NGS) techniques have recently been proven to be a powerful source of data to examine phylogenetic relationships at different taxonomic scales in Bromeliaceae (Machado et al., 2020; Paule et al., 2020; Chávez-Galarza et al., 2021a, 2021b; Loiseau et al., 2021; Möbus et al., 2021, Liu et al., 2022; Vera-Paz et al., 2022, 2023; Yardeni et al., 2022; Bratzel et al., 2023). Phylogenetic analyses based on complete plastome sequences derived from NGS have improved phylogenetic resolution and statistical support within the bromeliad subfamilies Puyoideae (Liu et al., 2022) and Tillandsioideae (Vera-Paz et al., 2022, 2023), when compared with previous single- and multilocus studies based on Sanger sequenced markers. Thus, plastome phylogenomics represents a promising alternative to address phylogenetic relationships among recently diverged lineages such as Hechtioideae.

The rapid advance of the NGS strategies has additionally improved our understanding of plant organelle evolution, particularly in plastid genomes. The plastome of land plants is highly conserved in terms of structure and gene content and order (Gao et al., 2010; Jansen & Ruhlman, 2012). It usually includes two single-copy regions, named large and small single copies (LSC and SSC, respectively), separated by two copies of an inverted repeat (IR; Palmer, 1991; Jansen & Ruhlman, 2012). Each land plant plastome contains approximately 80 protein-coding genes, 30 transfer RNA (tRNA) genes, and four ribosomal RNA (rRNA) genes (Mower & Vickrey, 2018). However, comparative analyses among closely related taxa across different land plant lineages have detected some deviations from this conserved structure, including expansion and contractions of the IR, sequence inversion, insertions and deletions, variations in the length of noncoding regions, and abundance of repetitive sequences (Palmer, 1991; Mower & Vickrey, 2018). Other frequent deviations are pseudogenization or loss of genes, commonly observed in the *ndh* gene family, where one to all the 11 genes that constitute this gene family have been lost or become nonfunctional across many lineages of the Streptophyta (Martín & Sabater, 2010; Strand et al., 2019; Yang et al., 2022).

In recent years, plastome comparative studies in Bromeliaceae have focused on describing from single (e.g., Nashima et al., 2015; Redwan et al., 2015; Poczai & Hyvönen, 2017; Chávez-Galarza et al., 2021a, 2021b) to several species (Paule et al., 2020; Möbus et al., 2021; Liu et al., 2022; Vera-Paz et al., 2022) representatives of the subfamilies Bromelioideae, Puyoideae, and Tillandsioideae, with 9, 13, and 37 sequenced species, respectively. A highly conserved plastome structure has generally been reported in Bromeliaceae (e.g., Redwan et al., 2015; Poczai & Hyvönen, 2017; Liu et al., 2022). However, structural rearrangements have been found in some species, including IR expansions in *Fascicularia bicolor* (Ruiz & Pavon) Mez and *Ochagavia carnea* (Beer) L.B.Sm. & Looser (Bromelioideae; Paule et al., 2020) and IR contractions in species of *Pseudoalcantarea* (Mez) Pinzón & Barfuss (Tillandsioideae; Vera-Paz et al., 2022). Furthermore, large inversions (ca. 27 kb) in the LSC of plastomes of species of *Vriesea* Lindl. (Tillandsioideae; Vera-Paz et al., 2022) have been identified. Given the plastome structural rearrangements recently discovered in other bromeliad lineages (Paule et al., 2020; Vera-Paz et al., 2022), we expect that the study of whole-plastome sequences from a representative sample of Hechtioideae could reveal new structural rearrangements and shed light on Hechtioideae plastome diversity and evolution.

In this study, we aim to (i) characterize plastome structural diversity in Hechtioideae; (ii) assess the utility of full plastomes for phylogenetic reconstruction; (iii) identify informative regions at different phylogenetic depths for future phylogenetic studies; and (iv) assess the evolution of selected plastome attributes across the obtained Hechtioideae phylogenetic tree.

2 Material and Methods

2.1 Taxon sampling, DNA extraction, and sequencing
We newly sequenced plastomes for 19 species of Hechtioideae, representing ca. 20% of its known species diversity and all currently recognized genera, including two species of *Bakerantha*, two species of *Mesoamerantha*, and 15 species of *Hechtia*. For further comparison with other bromeliad subfamilies, we newly sequenced *Pitcairnia breedlovei* L.B. Sm. (Pitcairnioideae) and *Puya mirabilis* (Mez) L.B. Sm.

(Puyoideae). Plastome sequences already available on GenBank representing species of Bromelioideae (*Ananas comosus* (L.) Merr., NC_026220.1; *Fascicularia bicolor*, MN563795.1; and *Ochagavia elegans* Phil., NC_045385.1) and Tillandsioideae (*Tillandsia usneoides* (L.) L., NC_045385.1) were also added to the taxon sampling. Additionally, we included the complete plastome sequence of *Typha latifolia* L. (Typhaceae; NC_013823) for rooting the phylogenetic tree. Voucher information of the sampled accessions can be found in Table S1.

Genomic DNA was extracted from fresh leaves collected from living plants deposited at the "Roger Orellana" Regional Botanical Garden at the "Centro de Investigación Científica de Yucatán (CICY)", Mexico. DNA was isolated using the cetyltrimethylammonium bromide method described by Doyle & Doyle (1987). DNA was quantified using the Quantus™ fluorometer (Promega Corporation, Madison, Wisconsin, USA) for a final concentration of 50 ng/μL. DNA integrity was assessed on 2% agarose gels stained with SYBR green and run for 45 min at 80 V. The library construction and whole-genome sequencing (WGS) were executed by RAPiD Genomics (Gainesville, Florida, USA). For this, the genomic DNA was fragmented with sonication to approximately 400 base pairs (bp). Library preparation used TrueSeq-like adapters, and sequencing was performed using Illumina HiSeq X Ten Systems (PE150).

2.2 Plastome assembly and annotation

Quality control of raw sequence reads was carried out using FastQC v.0.11.9 (Andrews, 2018). Raw reads were trimmed to remove adaptors and low-quality sequences using Trimmomatic v.0.39 (Bolger et al., 2014). Adapter removal and sequence quality were confirmed with FastQC. Reads were *de novo* assembled using GetOrganelle v.1.7.5 (Jin et al., 2020), applying a *K*-mer gradient (-*k* 21,45,65,85,105) suggested for 150 bp long paired data for assembling organelle genomes, up to 20 maximum extension runs, and using the default seed database (embplant_pt) to filter plastid reads. From the two naturally existing isomeric forms of the plastome (Palmer, 1983), we selected the one that matched the published plastome of *A. comosus* (NC_026220.1; Nashima et al., 2015). Assembly average coverage was evaluated by mapping the quality trimmed reads of each sample to the respective final sequence assembly using the BWA-MEM algorithm implemented in BWA v.0.7.17 (Li & Durbin, 2009) and using the "coverage" argument in SAMtools v.1.10 (Li et al., 2009; Table S2). Assembled plastomes were automatically annotated with Geneious Prime® v.2022.0.2 (Kearse et al., 2012) using the previously mentioned plastome of *A. comosus* and that of *Tillandsia utriculata* L. (NC_065191.1; Vera-Paz et al., 2022) as references. These two references were used to identify and corroborate the different genes that have been previously annotated for Bromeliaceae. Annotations of all protein-coding, tRNA, and rRNA genes were manually checked and, if needed, corrected in Geneious Prime®. tRNA genes annotations were confirmed with the online tRNAscan-SE v. 2.0 web server (Lowe & Chan, 2016; Chan & Lowe, 2019), and when necessary, borders predicted during automatic annotation were adjusted. Newly sequenced and assembled plastomes were deposited in GenBank under the accession numbers OQ818075–OQ818095 (Table S1). Plastome

circularization was performed with Geneious Prime®, and circular representations of the plastomes were drawn with OGDRAW v.1.3.1 (Lohse et al., 2013).

2.3 Comparative plastome analysis

For all the bromeliad plastomes, we compared gene content and order, the length (bp) of the full plastome, as well as that of the LSC, SSC, and IR, and the guanine–cytosine (GC) content (%) of the same regions using Geneious Prime®. Genes on the boundaries of the junction sites of the IR and single-copy regions were visualized in IRscope (Amiryousefi et al., 2018). Since several differences were observed in the *ndh* gene family among Hechtioideae species, we carefully inspected for gene loss and potential pseudogenization. To corroborate point base substitutions and indel events (insertion and deletions), reads were mapped back to gene contigs and the resulting read mapping files were visualized using Tablet v.1.21.02.08 (Milne et al., 2013), evaluating the assembly accuracy and contig coverage. Here, we considered (i) potential gene pseudogenization when point base substitutions caused premature stop-codons; (ii) potential gene pseudogenization due to indel events causing premature stop-codons; and (iii) gene loss when the gene sequence was completely absent in the plastid genome. To visualize *ndh* gene family changes across the phylogeny, we labeled species that have each of the three above-mentioned cases.

2.4 Phylogenetic analyses

To assess the utility of full plastomes for phylogenetic reconstruction, we analyzed plastome sequences of the 25 sampled bromeliad taxa plus *Typha latifolia* for rooting the tree. Plastome sequences were automatically aligned with the MAFFT v.7.487 (Katoh & Standley, 2013) plugin of Geneious Prime®. One IR region was excluded to avoid duplication of data for phylogenetic analyses. Poorly aligned and divergent regions were identified with Gblocks v.0.91b (Castresana, 2000) and excluded with the -E flag of RAxML v.8.2.10 (Stamatakis, 2014). Regions corresponding to small inversions (<200 pb) detected across different species and one large inversion of 3.9 kb identified in *H. deceptrix* were also excluded from phylogenetic analyses. Alignments of the complete plastomes and the final alignment used in the phylogenetic analysis are available as supplementary information S1. A maximum likelihood (ML) phylogenetic analysis was performed using RAxML applying the GTR + G model. One hundred searches for the best ML tree were performed and clade support was assessed with 1000 bootstrap replicates. Node support was drawn on the best ML tree. The ML analysis was performed in the CIPRES Science Gateway service (Miller et al., 2010).

2.5 Phylogenetic informativeness (PI)

We performed a PI analysis (Townsend, 2007) to evaluate the utility of the recovered plastid regions in resolving deep and shallow phylogenetic divergences in Hechtioideae. For this, the best ML tree was converted into ultrametric with the function "chronopl" of the APE v.5.6-2 package ($\lambda = 0.0$; Paradis & Schliep, 2019) in R v.4.1.2 (R Core Team, 2022), applying a relative time scale where the tree tips correspond to time 0 and the root to time 1. Using as input individual

alignments of each exon, intron, and IGS, site substitution rates, and net PI profiles were calculated in TAPIR (Pond et al., 2005; Faircloth et al., 2012). Net PI profiles were plotted for each partition and contrasted against the ultrametric tree. Maximum net PI was recorded for each partition, as well as the time at which these values were reached. Markers were ranked according to their maximum net PI to select a set of regions that would potentially be most informative for resolving phylogenetic relationships within Hechtioideae.

2.6 Ancestral state reconstruction (ASR) and evolutionary shifts of plastome attributes

ASR analysis was performed in R for eight continuous plastome attributes, including size and GC content of the full plastome and of its three structural regions (i.e., LSC, SSC, and IR; Table S3). Using the "fastAnc" function of the package *phytools* v.1.2-0 (Revell, 2012), nodes' ancestral states, variances, and their 95% confidence intervals (CIs) were inferred under a ML framework. Values of the analyzed attributes were mapped to the ultrametric tree using the "contMap" function of *phytools*.

The presence of evolutionary rate shifts of the analyzed plastome attributes was assessed both across the temporal scale and among lineages. Raw values obtained of the plastome traits were transformed into a logarithmic scale to reduce heterogeneity and used as input data. An analysis of phenotypic evolution was performed in the Bayesian Analysis of Macroevolutionary Mixtures (BAMM v.2.5.0) program (Rabosky, 2014), which estimates changes in evolutionary rates under a compound Poisson process along the phylogeny and then evaluates models that present variation in the number of evolutionary rate shifts of the phenotypic attributes using a reversible Markov Chain Monte Carlo (rjMCMC). Adequate priors were obtained with the R package *BAMMtools* v.2.1.10 (Rabosky, 2014) and the selected priors were used to run BAMM analyses with 20 million generations. Chain convergence was examined with the package *coda* (Plummer et al., 2006) and an Effective Sample Size (ESS) of the MCMC ≥ 200 was ensured. BAMM output was analyzed with *BAMMtools* in R to extract the number and probability of shifts in the evolutionary rate for each plastome attribute. Maximum a posteriori probability (MAP) configuration was generated when a shift or set of shifts were detected, to visualize the number and location of the shifts. The analysis of phenotypic evolution performed in this study differs from the diversification analysis typically performed in BAMM and does not require accounting for incomplete taxon sampling. Furthermore, we have included representatives from all the main clades of Hechtioideae to represent plastome diversity at the subfamily level.

3 Results

3.1 Plastome attributes in the newly sequenced Bromeliaceae

Plastome sizes in the outgroup species *Pitcairnia breedlovei* and *Puya mirabilis* were 160 896 and 159 830 bp, respectively. The plastomes of Hechtioideae range from 155 133 bp (*H. aquamarina* I. Ramírez & C.F. Jiménez) to 165 394 bp (*H. deceptrix*) in length. All newly sequenced plastomes had a typical quadripartite structure (Figs. 1, S1), including a LSC region slightly varying in length from 85 823 bp (*H. iltisii* Burt-Utley & Utley) to 88 802 bp (*P. breedlovei*), and a SSC region substantially reduced in length in *H. deceptrix* with 8600 bp, and the rest of the species ranging from 14 961 bp (*H. michoacana* Burt-Utley, Utley & García-Mend.) to 18 642 bp (*M. guatemalensis* (Mez) I. Ramírez & K. Romero). The single-copy regions are separated by two copies of an IR ranging from 25 606 bp (*H. aquamarina*) to 34 652 bp (*H. deceptrix*; Tables 1 and S3) in length. The total GC content of the newly sequenced plastomes ranged from 37.04% to 37.43%, while the GC content ranged from 35.04% to 35.44% in the LSC, from 30.44% to 31.58% in the SSC, and from 40.09% to 42.98% in the IRs (Table S3).

The plastomes of *P. breedlovei* and *Puya mirabilis* contain 115 unique coding genes, with 81 protein-coding genes, 30 tRNA genes, and four rRNA genes (Table 2). Each IR region contains 22 genes, including eight complete (*ndhB*, *rpl2*, *rpl23*, *rps7*, *rps19*, *ycf2*, *ycf15*, and *ycf68*) and two partial (*rps12* and *ycf1*) protein-coding genes, eight tRNA genes ($trnA^{UGC}$, $trnH^{GUG}$, $trnI^{CAU}$, $trnI^{GAU}$, $trnL^{CAA}$, $trnN^{GUU}$, $trnR^{ACG}$, and $trnV^{GAC}$), and four rRNA genes (*rrn4.5S*, *rrn5S*, *rrn16S*, and *rrn23S*). Gene content of the sequenced Hechtioideae plastomes, in general, follows that described above for *P. breedlovei* and *Puya mirabilis*, except for the following cases. We detected an IR expansion in *H. deceptrix*, in which the complete *ycf1*, *rps15*, *ndhH*, and a partial *ndhA* genes are embedded within the IR (Fig. S1). Conversely, *H. aquamarina*, *H. mooreana* L.B. Sm., and *H. stenopetala* Klotzsch show an IR contraction, where the complete *ycf1* gene has been translocated to the SSC (Figs. 2, S1, S2). Furthermore, four *ndh* genes presented point mutations causing premature stop codons in at least one species of Hechtioideae, all tagged as potential pseudogenes (Fig. 3). Eight additional *ndh* genes (*ndhA*, *ndhC*, *ndhD*, *ndhE*, *ndhF*, *ndhH*, *ndhI*, and *ndhK*) were identified as potential pseudogenes as they presented base deletions in some species of *Hechtia* (Fig. 3), losing between one (mostly in mononucleotide repeat regions) and several base pairs (ca. 95%) relative to the functional genes, while others presented base insertions ranging from one to seven bases that affect the reading frame. Three genes of the *ndh* family were recorded as absent in different *Hechtia* species, including *ndhA* (*H. confusa* L.B. Sm.), *ndhH* (*H. pringlei* B.L. Rob. & Greenm.), and *ndhJ* (*H. aquamarina*, *H. colossa* Mart.-Correa, Espejo & López-Ferr., *H. iltisii*, *H. mooreana*, and *H. stenopetala*). Other potential pseudogenes include the truncated *ycf1* gene at the SSC/IRb junction and the *ycf15* gene. Gene order is in general highly conserved in the sampled species of Hechtioideae as has been previously reported for Bromeliaceae, with the following exception. Changes in gene order in the SSC were found in *H. deceptrix*, which has a 3966 bp long inversion spanning genes *ndhF* to *ccsA*, and part of its flanking IGS.

Differences were detected in the SSC/IRa junction, where most of the Hechtioideae species have the *ycf1* gene, except for *H. aquamarina*, *H. mooreana*, and *H. stenopetala*, which instead have a truncated *ndhF* gene at this region following an IR contraction of these species. The SSC/IRb junction varied more widely. Over this junction, the following cases were detected: (i) a *ycf1* pseudogene of variable size
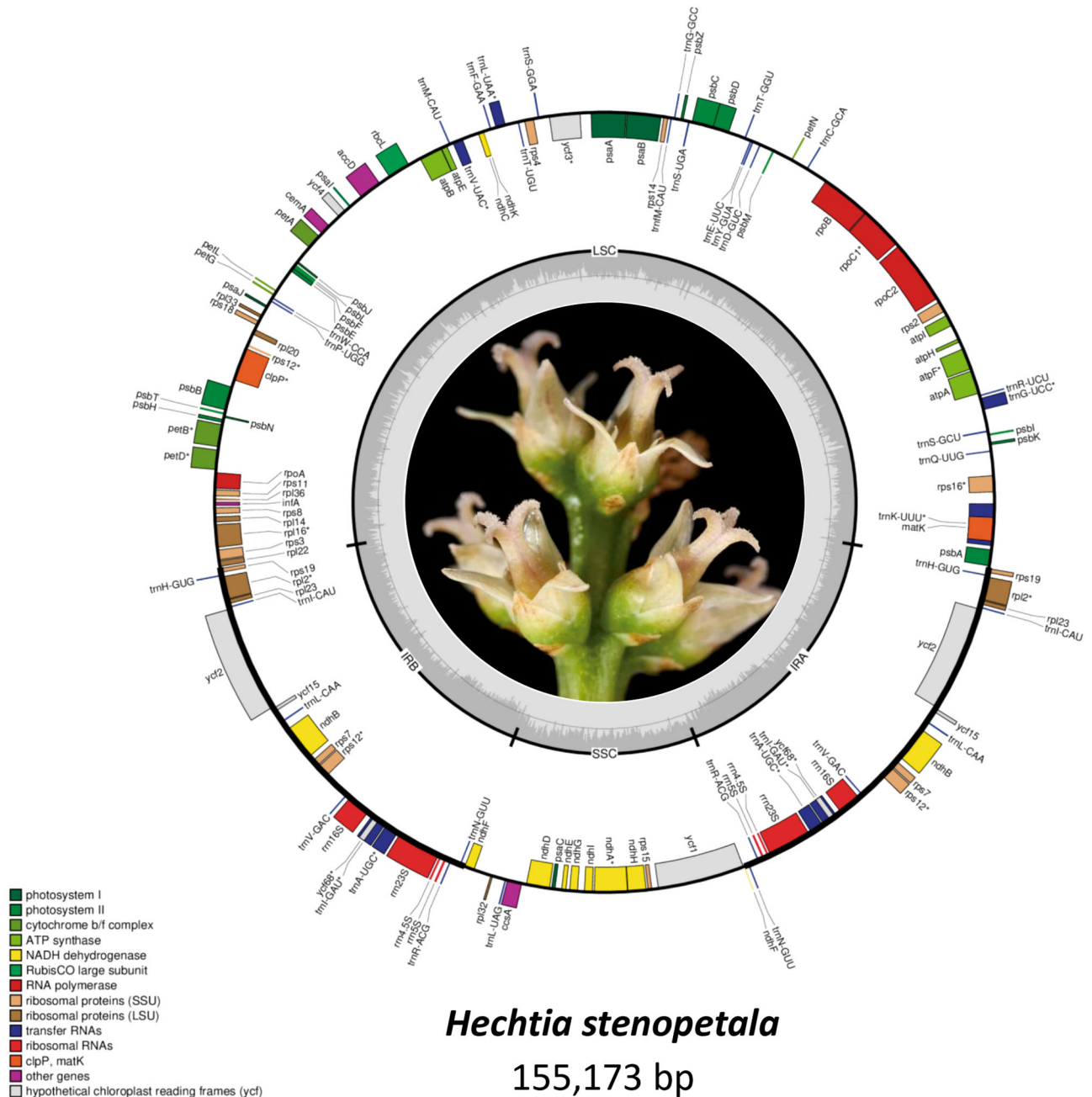
Fig. 1. Circular representation of the *Hechtia stenopetala* plastome. The color depicted in the genes represents their functional category. The innermost gray circle denotes the guanine–cytosine content across the genome. Genes that are transcribed counter-clockwise and clockwise are presented to the outside and the inside of the outer circle, respectively. Genes with introns are marked with an asterisk. Photograph by G. Romero-González.

(1076–2393 bp; Figs. 2, S2) partially overlapping with the *ndhF* gene, (ii) the *ycf1-ndhF* IGS, (iii) the *ndhA* gene due to an important IR expansion in *H. deceptrix*, and (iv) a *ndhF* pseudogene due a small IR contraction in *H. aquamarina*, *H. mooreana*, and *H. stenopetala* (Figs. 2, S2).

3.2 Phylogenetic analysis
After the exclusion of one IR, ambiguously aligned regions, and inversions, the final alignment used for phylogenetic

inference was 126 621 bp long, including 63 871 pb corresponding to protein-coding genes, 6726 pb to RNA genes, 16 086 pb to introns, and 39 938 pb to IGS. The ML analysis retrieved a tree where all, except the below noted nodes, are strongly supported (BS ≥ 85; Figs. 3, S3). In this tree, *T. usneoides* is the sister species of the remaining bromeliad lineages, which are further divided into two main clades. The first main clade includes *P. breedlovei* as sister of *Puya mirabilis* plus a clade including all Bromelioideae representa-

Table 1 Comparison of the characteristics of the newly sequenced and assembled Bromeliaceae plastomes

Subfamily	Taxon	Total plastome length (bp)	LSC length (bp)	SSC length (bp)	IR length (bp)	Total plastome GC% content	No. of protein-coding genes	No. of tRNA genes	No. of rRNA genes
Hechtioideae	*Bakerantha purpusii*	160 292	88 075	18 601	26 808	37.30	81	30	4
Hechtioideae	*Bakerantha tillandsioides*	158 414	86 175	18 629	26 805	37.43	81	30	4
Hechtioideae	*Hechtia aquamarina*	155 133	85 856	18 065	25 606	37.35	80	30	4
Hechtioideae	*Hechtia colossa*	157 929	85 918	18 521	26 745	37.25	80	30	4
Hechtioideae	*Hechtia confusa*	157 118	87 600	16 030	26 744	37.31	80	30	4
Hechtioideae	*Hechtia deceptrix*	165 394	87 490	8600	34 652	37.04	81	30	4
Hechtioideae	*Hechtia elliptica*	159 395	87 415	18 562	26 709	37.32	81	30	4
Hechtioideae	*Hechtia iltisii*	157 935	85 823	18 574	26 769	37.28	80	30	4
Hechtioideae	*Hechtia matudae*	159 490	87 530	18 430	26 765	37.30	81	30	4
Hechtioideae	*Hechtia michoacana*	158 254	87 241	14 961	28 026	37.37	81	30	4
Hechtioideae	*Hechtia mooreana*	155 203	85 923	18 066	25 607	37.34	80	30	4
Hechtioideae	*Hechtia myriantha*	159 657	87 711	18 516	26 715	37.30	81	30	4
Hechtioideae	*Hechtia podantha*	158 441	87 562	18 393	26 243	37.27	81	30	4
Hechtioideae	*Hechtia pringlei*	156 758	87 512	15 818	26 14	37.28	80	30	4
Hechtioideae	*Hechtia rosea*	158 828	87 280	17 372	27 088	37.32	81	30	4
Hechtioideae	*Hechtia schottii*	159 488	87 439	18 561	26 744	37.30	81	30	4
Hechtioideae	*Hechtia stenopetala*	155 173	85 886	18 065	25 611	37.35	80	30	4
Hechtioideae	*Mesoamerantha guatemalensis*	160 022	87 632	18 642	26 874	37.35	81	30	4
Hechtioideae	*Mesoamerantha malvernii*	160 034	87 839	18 625	26 785	37.43	81	30	4
Pitcairnioideae	*Pitcairnia breedlovei*	160 896	88 802	18 568	26 763	37.16	81	30	4
Puyoideae	*Puya mirabilis*	159 830	87 801	18 529	26 750	37.30	81	30	4

GC content, guanine–cytosine content; IR, inverted repeat; LSC, large single copy; rRNA genes, ribosomal RNA genes; SSC, small single copy; tRNA genes, transfer RNA genes.

Table 2 Plastid genes and their functional groups of the newly sequenced and annotated Bromeliaceae species

Function	Group of genes	Genes
Protein synthesis and DNA replication	Ribosomal protein small subunit	*rps2, rps3, rps4, rps7* (×2), *rps8, rps11, rps12*,[†] (×2), *rps14, rps15* (×2[†]), *rps16*,* *rps18, rps19* (×2)
	Ribosomal protein large subunit	*rpl2** (×2), *rpl14, rpl16,** *rpl20, rpl22, rpl23* (×2), *rpl32, rpl33, rpl36*
	Subunits of RNA polymerase	*rpoA, rpoB, rpoC1,* *rpoC2*
	Ribosomal RNAs	*rrn4.5S* (2), *rrn5S* (×2), *rrn16S* (×2), *rrn23S* (×2)
	Transfer RNAs	*trnA*^{UGC}* (×2), *trnC*^{GCA}, *trnD*^{GUC}, *trnE*^{UUC}, *trnF*^{GAA}, *trnfM*^{CAU}, *trnG*^{GCC}, *trnG*^{UCC},* *trnH*^{GUG} (×2), *trnI*^{CAU} (×2), *trnI*^{GAU}* (×2), *trnK*^{UUU},* *trnL*^{CAA} (×2), *trnL*^{UAA},* *trnL*^{UAG}, *trnM*^{CAU}, *trnN*^{GUU} (×2), *trnP*^{UGG}, *trnQ*^{UUG}, *trnR*^{ACG} (×2), *trnR*^{UCU}, *trnS*^{GCU}, *trnS*^{GGA}, *trnS*^{UGA}, *trnT*^{GGU}, *trnT*^{UGU,} *trnV*^{GAC} (×2), *trnV*^{UAC},* *trnW*^{CCA}, *trnY*^{GUA}
Photosynthesis	ATP synthase	*atpA, atpB, atpE, atpF,* *atpH, atpI*
	Cytochrome b/f complex	*petA, petB,* *petD,* *petG, petL, petN*
	Large subunit Rubisco	*rbcL*
	NADH dehydrogenase	*ndhA** (×2[‡]), *ndhB** (×2), *ndhC, ndhD, ndhE, ndhF, ndhG, ndhH* (×2[‡]), *ndhI, ndhJ, ndhK*
	Photosystem I	*psaA, psaB, psaC, psaI, psaJ*
	Photosystem II	*psbA, psbB, psbC, psbD, psbE, psbF, psbH, psbI, psbJ, psbK, psbL, psbM, psbN, psbT, psbZ*
Other genes	Acetyl-CoA-carboxylase	*accD*
	ATP-dependent protease	*clpP*[§]
	Cytochrome *c* biogenesis	*ccsA*
	Inner membrane protein	*cemA*
	Maturase	*matK*
	Translation initiation factor	*infA*
Protein transport through plastid membranes	Conserved hypothetical plastome ORF	*ycf1* (×2), *ycf2* (×2)
Potentially involved in the assembly of photosystem I	Conserved hypothetical plastome ORF	*ycf3,*[†] *ycf4*
Unknown function	Conserved hypothetical plastome ORF	*ycf15* (×2), *ycf68** (×2)

*Genes with one intron; [†]Trans-spliced gene; [‡]Only duplicated in *Hechtia deceptrix*; [§]Genes with two introns.

tives. Within Bromelioideae, *A. comosus* is sister to a lineage including *O. elegans* plus *F. bicolor*. The second main clade corresponds to Hechtioideae, including the three currently recognized genera as monophyletic. *Mesoamerantha* (clade C sensu Ramírez-Morillo et al., 2018a) is sister to a clade including *Bakerantha* (clade B) and *Hechtia*. In *Hechtia, H. myriantha* Mez is recovered as the sister lineage of all remaining species, which are further divided into two clades equivalent to the clades D–E (BS = 52) and F of Ramírez-Morillo et al. (2018a). Clades D–E include *H. deceptrix* as sister of a clade composed of *H. schottii* Baker and *H. elliptica* L.B. Sm., while clade F is further divided into two clades. In the first one, *H. colossa* is sister of a clade containing the [*H. matudae* L.B. Sm. + *H. michoacana*] and [*H. iltisii* + *H. podantha* Mez] clades. In the second clade, *H. rosea* É. Morren ex Baker is the successive sister of *H. confusa, H. pringlei, H. aquamarina*, and a clade of *H. mooreana* and *H. stenopetala* (Figs. 3, S3).

3.3 PI of plastid regions
The PI profiles showed that most of the loci reached their maximum net PI toward time 60 of our arbitrary scale. Some

IGS and introns reached their maximum net PI near time 1 at shallow phylogenetic divergences (Fig. 4A; Table S4), while most of the coding genes presented their maximum net PI at deeper evolutionary depths (between time 6 and 99). The median of the maximum net PI was higher for introns (0.32), followed by IGS (0.19) and coding genes (8.4×10^{-2}; Fig. 4B). Among coding genes, the maximum net PI ranged from 3.2×10^{-3} in the exon 1 of the *ycf68* gene to 3.8 in the *ycf1* gene. The maximum net PI of IGS ranged from 4.4×10^{-3} in *trnI-rpl23* IGS to 2.7 in *trnT-psbD* IGS, while in introns, it varied between 1.4×10^{-2} in the *rps12* intron and 1.2 in the *atpF* intron. The 10 most informative loci in this study were the *ycf1* gene, the intergenic spacers *trnT-psbD, trnS-trnG, psbE-petL,* and *rps16-trnQ*, the *rpoC2* gene, the *ndhC-trnV* IGS, the *atpF* and *rpl16* introns, and the *rpoB-trnC* IGS (listed in order of informativeness).

3.4 ASR of plastome attributes
The crown node of Hechtioideae was reconstructed with a plastome size of 159 640.88 bp (95% CI = 155 397.94–163 883.81 bp), while the LSC, IR, and SSC sizes were 87 415.88 bp (95% CI = 85 150.8–89 680.96 bp), 27 004 bp
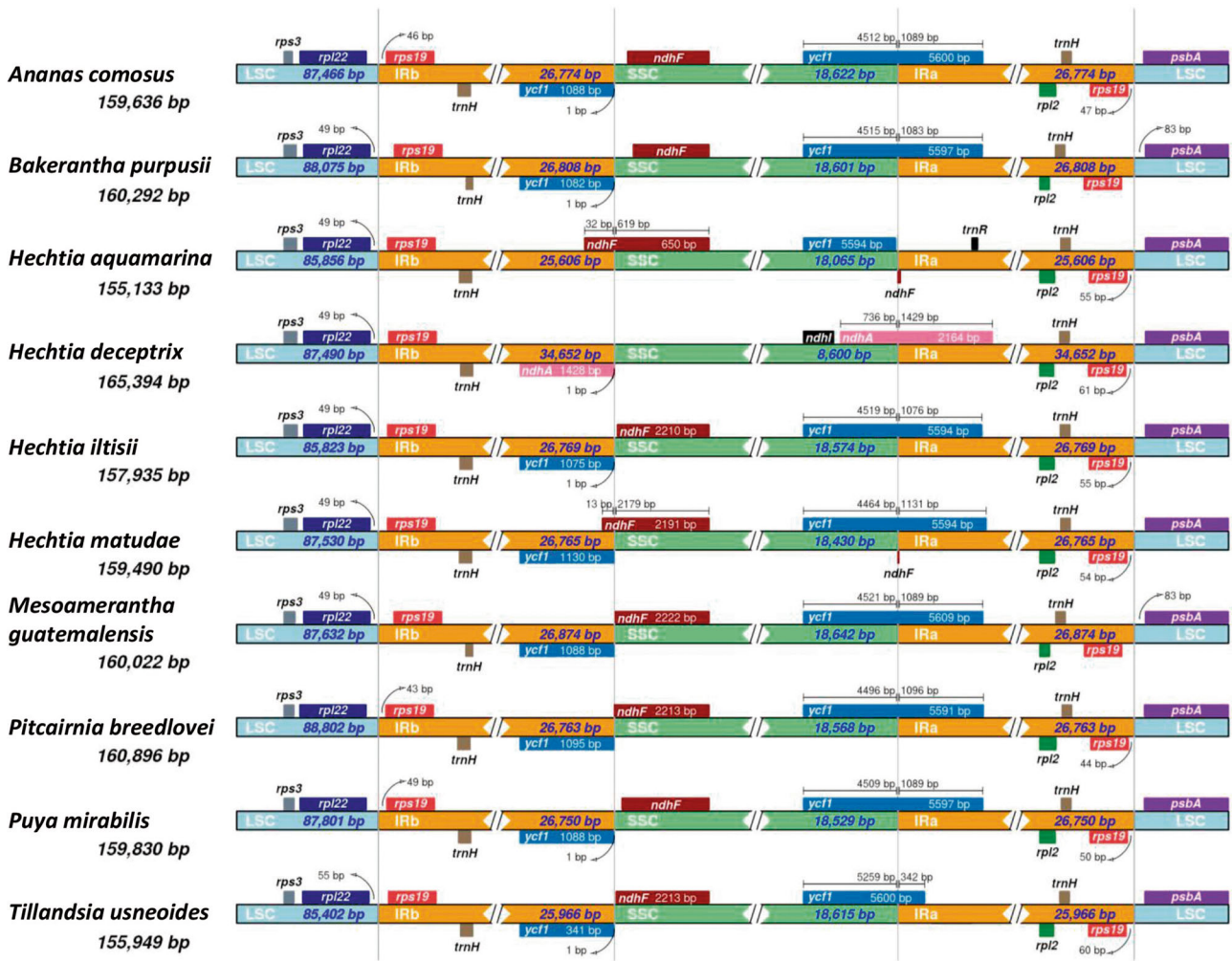
Fig. 2. Comparison of the large single copy (LSC), small single copy (SSC), and inverted repeat (IR) borders showing the most frequent variations found in Hechtioideae species and other bromeliad plastomes used for comparison. Genes shown above and below the lines are transcribed clockwise and counter-clockwise, respectively.

(95% CI = 22 787.82−31 220.19 bp), and 18 217 bp (95% CI = 12 422.15−24 011.84 bp), respectively. The total plastome GC content for the same node was estimated to be 37.33% (95% CI = 37.14%−37.52%), while the LSC, IR, and SSC GC contents were 35.30% (95% CI = 35.16%−35.45%), 42.62% (95% CI = 41.25%−44%), and 31.40% (95% CI = 30.5%−32.31%), respectively. The estimation of the ASR, variance, and 95% CIs for the eight plastome attributes in each node for the retrieved phylogenetic context can be found in Table S5.

Shifts in phenotypic evolutionary rates were only found in characteristics involving the IR and SSC regions. The clade F and *H. deceptrix* presented rate shifts in three out of the four attributes (Fig. 5). Three rate shifts were detected for the SSC size (high posterior probabilities [HPP] = 0.38) at the *F. bicolor*−*O. elegans* and *Hechtia* F clades, as well as in *H. deceptrix* (Fig. 5A). A single evolutionary rate shift was detected for the SSC GC content (HPP = 0.52) at a subclade of clade F (Fig. 5B), including *H. rosea*, *H. confusa*, *H. pringlei*, *H. aquamarina*, *H. mooreana*, and *H. stenopetala*. IR size presented four different rate shifts (HPP = 0.77) at *T. usneoides*, *F. bicolor*, *H. deceptrix*, and the *Hechtia* clade F

(Fig. 5C), whereas only three rate shifts were detected for IR GC content (HPP = 0.52) at *F. bicolor*, *H. deceptrix*, and *Hechtia* clade F (Fig. 5D).

4 Discussion

4.1 Plastome features in Hechtioideae
Study of whole-plastome sequences from Hechtioideae representatives revealed new structural rearrangements in the plastid genome of bromeliad family and shed light on Hechtioideae plastome structure evolution. Genome sizes of the *de novo* assembled bromeliads plastomes (Tables 1, S3) were generally within the range previously reported for the family (Paule et al., 2020; Liu et al., 2022; Vera-Paz et al., 2022), ranging between 140 and 160 kb, except for *H. deceptrix* (165 394 bp), which has the largest plastome reported so far in the family. Additionally, the SSC (8600 bp) and IR (34 652 bp) regions in *H. deceptrix* are the smallest and the largest, respectively, compared with those previously reported for other bromeliad plastomes (e.g., Redwan et al., 2015;
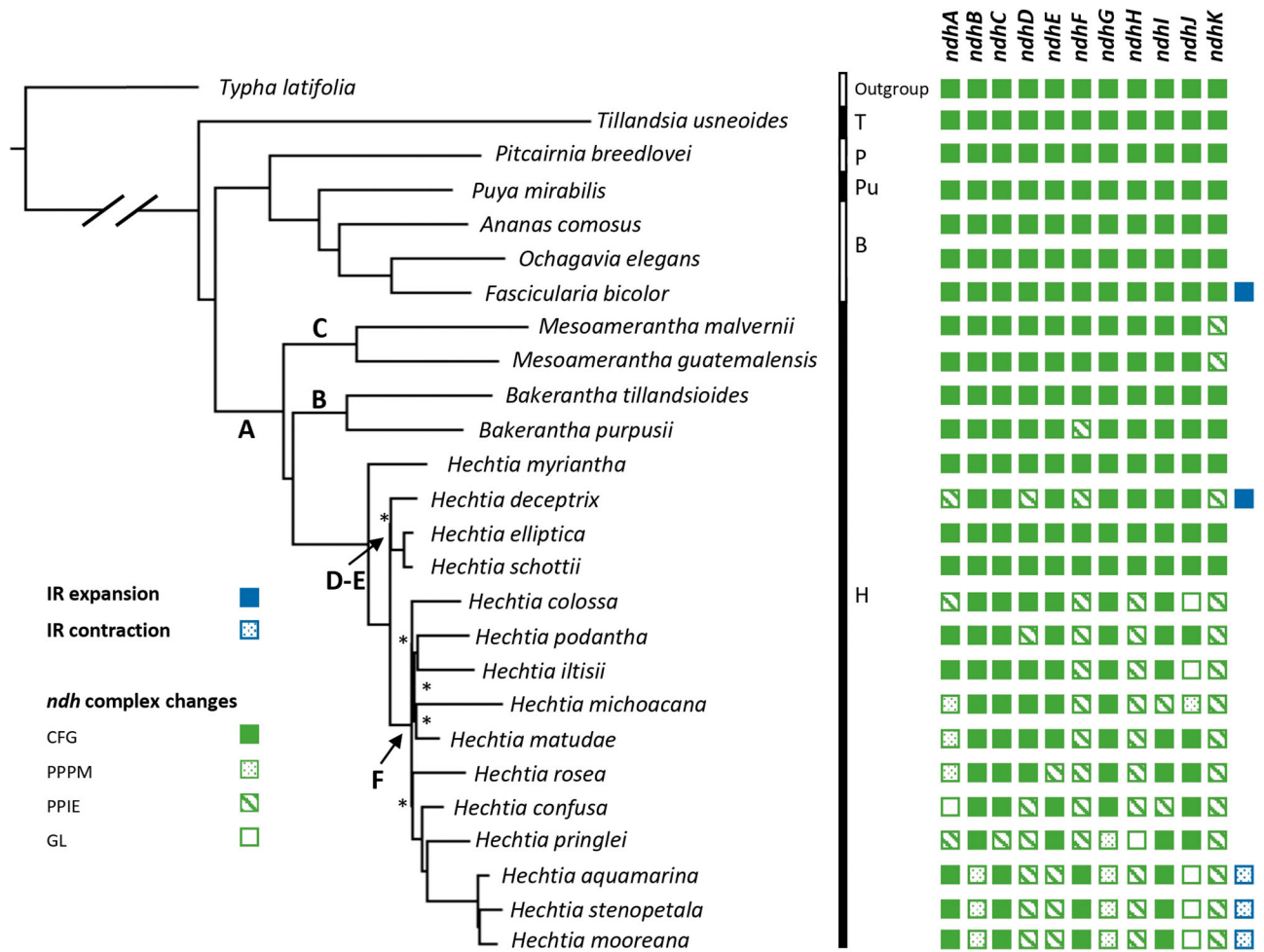
Fig. 3. Plastid structural changes mapped on a maximum likelihood tree based on the analysis of 26 complete bromeliad plastomes. Changes found on the *ndh* gene family are depicted by green squares, while expansions and contractions of the IR are shown by blue squares. Abbreviations for *ndh* gene changes: CFG, complete functional gene; GL, gene loss; PPIE, potential pseudogenization by indel events; PPPM, potential pseudogenization by point mutation. Capital letters at the nodes represent clades identified by Ramírez-Morillo et al. (2018a). Nodes with BS < 85% are denoted by an asterisk. Abbreviations for clade names: B, Bromelioideae; BS, bootstrap support; H, Hechtioideae; P, Pitcairnioideae; Pu, Puyoideae; T, Tillandsioideae.

Paule et al., 2020; Liu et al., 2022; Vera-Paz et al., 2022). These variations in the attributes of the plastome of *H. deceptrix* can largely be attributed to an IR expansion and consequent duplication of genes normally present as single copy. Small-sized plastomes in Hechtioideae (155 kb), present in *H. aquamarina*, *H. mooreana*, and *H. stenopetala*, follow a small IR contraction, potential gene pseudogenization (by base deletion), and gene loss (Fig. 3). Differences in plastome size have been reported across land plants (Mower & Vickrey, 2018) associated to variations in the length of noncoding regions, abundance of repetitive sequences, IR expansions or contractions, gene duplication, and gene and intron loss (Gao et al., 2010; Jansen & Ruhlman, 2012; Yang et al., 2022).

As previously reported for other bromeliad lineages, gene content in Hechtioideae is highly conserved, except for some taxa lacking certain genes of the *ndh* family (see discussion below). Additionally, the annotated *ycf15* and *ycf68* genes reported here have inconsistently been annotated in other

Bromeliaceae lineages (see Vera-Paz et al., 2022 vs. Liu et al., 2022), albeit these two genes are indeed present in all bromeliad representatives sequenced so far. Despite the overall gene content conservation, events of inversion, gene loss, and duplication were found to alter gene order in the genus *Hechtia* relative to the other Hechtioideae. A large inversion ca. 3.9 kb in the SSC region including four full protein-coding genes (*ndhF*, *rpl32*, *trnL*, and *ccsA*) was found in *H. deceptrix*. Large sequence inversions in Bromeliaceae were previously reported for the *T. biflora* Ruiz & Pav. complex (2.2 kb) and *Vriesea* species (28 kb), involving one and 24 genes, respectively, from the LSC region (Vera-Paz et al., 2022), suggesting large inversions as a common structural rearrangement in the family.

Differences at the SSC/IR junction were found among Hechtioideae species, including a ca. 7 kb expansion of the IR in *H. deceptrix*, where three full coding genes (*ycf1*, *rps15*, and *ndhH*) and one partial gene (*ndhA*) are translocated from the SSC to the IR, and a small IR reduction (600 bp) in
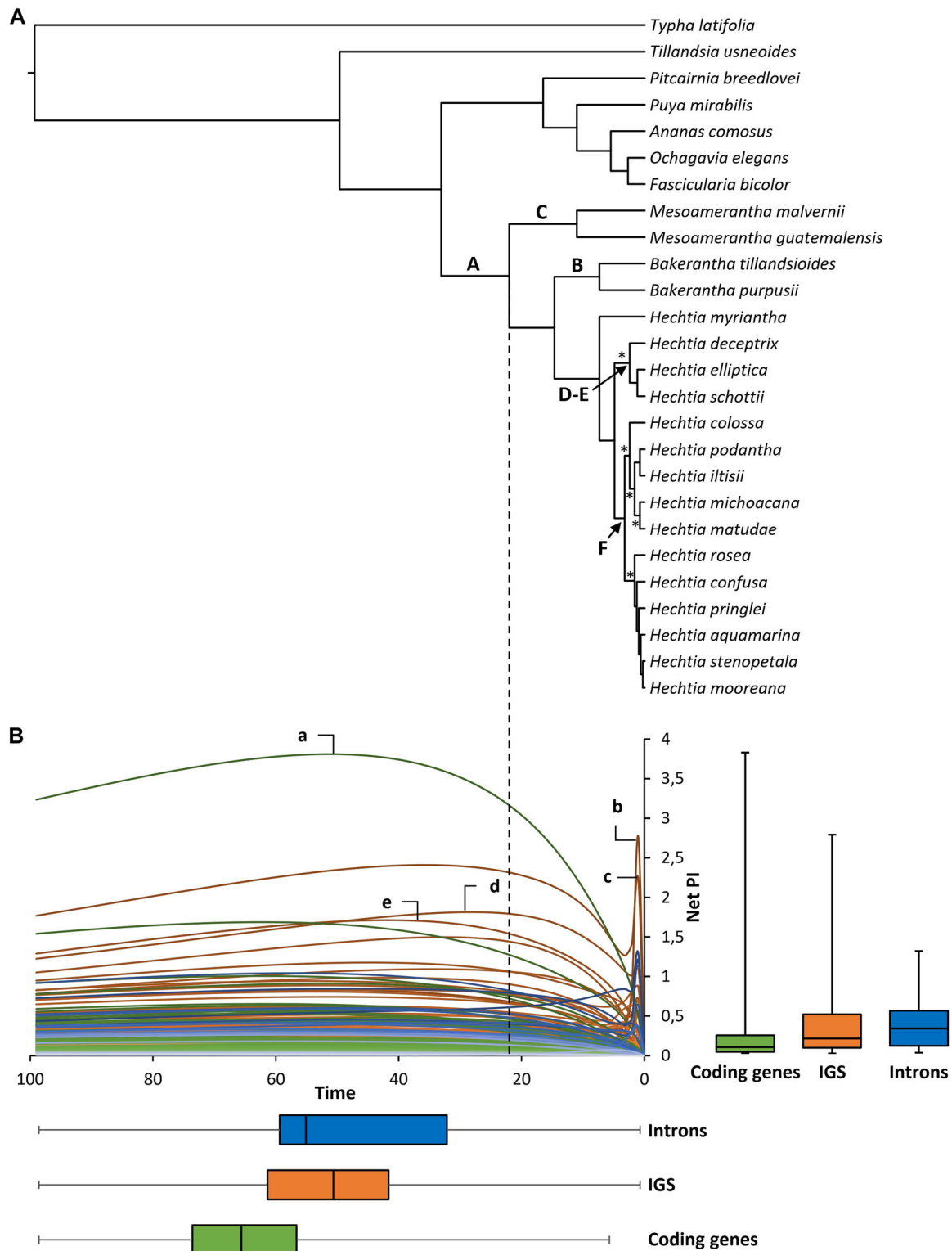
Fig. 4. A, The obtained maximum likelihood (ML) tree with branch lengths converted into ultrametric. **B,** Net phylogenetic informativeness (PI) profiles of plastid coding genes (green), intergenic spacers (blue), and introns (orange). Lowercase letters represent the five loci with the highest PI values: (a) *ycf1*, (b) *trnT^GGU*–psbD, (c) *trnS^GCU*–*trnG^UCC*, (d) *psbE*–*petL*, and (e) and *rps16*–*trnQ^UUG*. Whiskers denote the maximum and minimum values. The arbitrary time scale of the PI profiles matches the one of the ultrametric tree in (A).
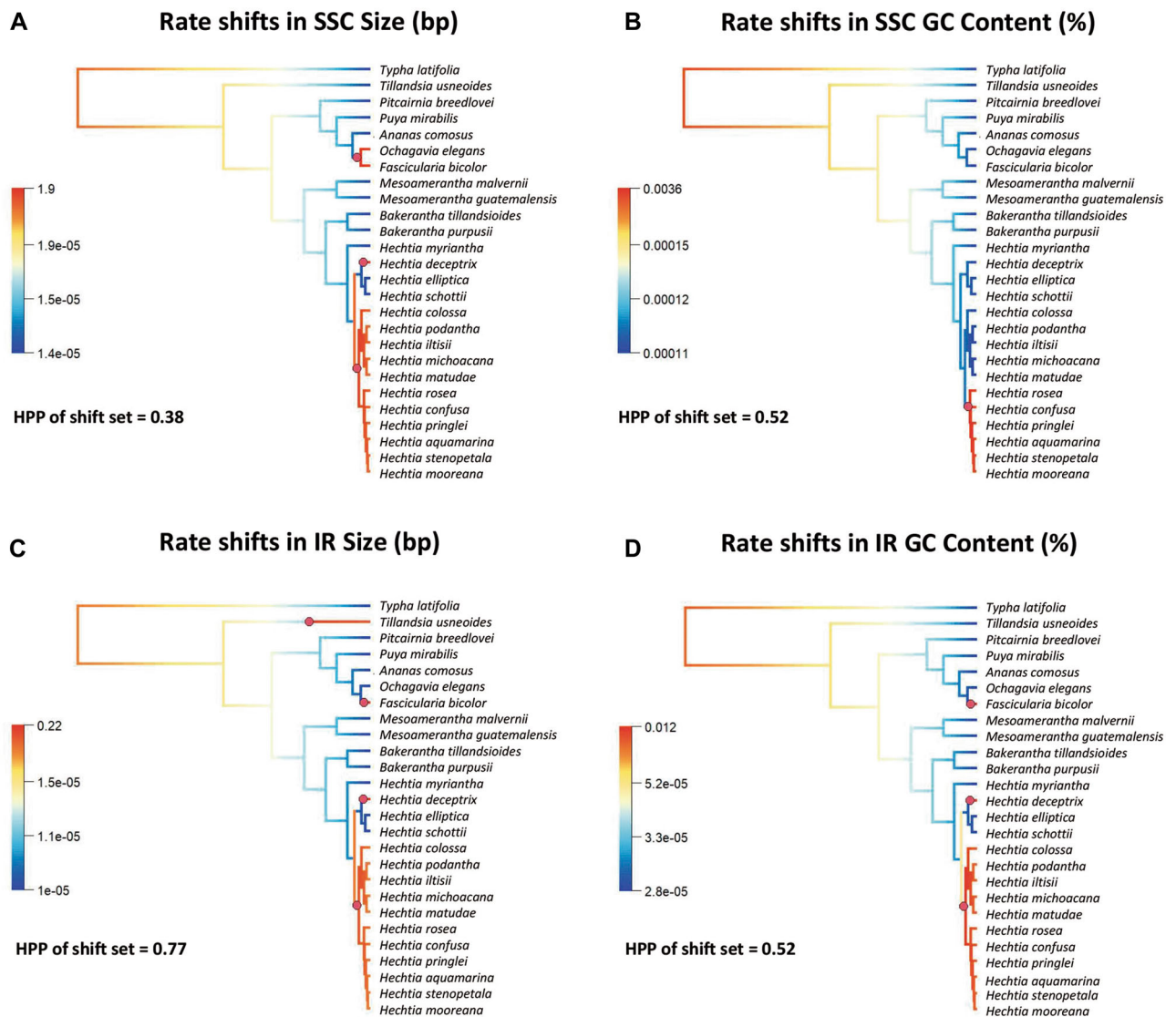
Fig. 5. Evolution of four plastome attributes where evolutionary rate shift sets were detected by BAMM with posterior probabilities ≥ 0.5. **A**, SSC size. **B**, SSC GC content. **C**, IR size. **D**, IR GC content. Red dots indicate the location of detected evolutionary rate shifts. GC, guanine–cytosine; HPP, highest posterior probability; IR, inverted repeat; SSC, small single copy.

H. aquamarina, *H. mooreana*, and *H. stenopetala*, where the portion of the *ycf1* gene located in other species in the IRa is transferred to the SSC, so that the entire *ycf1* gene is included in the SSC (Figs. 2, 3, S2). The latter rearrangement led to the absence of the *ycf1* pseudogene in the SSC/IRb border annotated in other Hechtioideae species; however, if indeed the *ycf1* pseudogene is not functional, this change should not affect the overall gene dosage. In other bromeliad lineages, expansions and contractions of the IR have instead involved the LSC/IR junction, such as the IR expansion of *F. bicolor* and *O. carnea* (Bromelioideae; Paule et al., 2020), and a large IR contraction in *Pseudalcantarea* species (Tillandsioideae; Vera-Paz et al., 2022). In the case of Hechtioideae species, the LSC/IR junction is located between the *rps19* and *rpl22* genes, as in other Poales lineages (Wang et al., 2008). Changes in IR boundaries have occurred

multiple times at different evolutionary depths in land plants, causing the transfer of multiple genes in or out of the IR (Zhu et al., 2016), with those related to IR expansions being the most common (Mower & Vickrey, 2018).

In some Hechtioideae species, one or more of the 11 *ndh* genes have undergone potential pseudogenization (Fig. 3). Possible gene pseudogenization in Hechtioideae is caused by point mutations or by a series of small base deletions or insertions that might not allow the final translation into proteins, making the genes potentially nonfunctional, as has been reported for *Pinus* spp. or some nonphotosynthetic parasitic plants (Martín & Sabater, 2010). Potential pseudo-genization involving the *ndh* gene family has only been reported in Bromeliaceae for species of *Pseudoalcantarea*, where one of the two *ndhB* copies is truncated at the LSC/IRb border due to a large IR contraction (Vera-Paz et al., 2022).

In Hechtioideae, the most recently diverged species of *Hechtia* are the ones presenting most cases of *ndh* family gene loss and/or potential pseudogenization, particularly in clade F (Fig. 3). However, potential pseudogenization or loss of the *ndh* genes appears to occur independently across the Hechtioideae phylogenetic tree, as has been reported for several land plant lineages (Martín & Sabater, 2010; Barrett et al., 2019; Strand et al., 2019; Yang et al., 2022). Future studies aimed at obtaining transcriptomic data could help to assess whether the genes of the *ndh* family identified as potential pseudogenes in Hechtioideae species are indeed not expressed.

In some *Hechtia* species, the *ndhA*, *ndhH*, and *ndhJ* genes are absent. The loss of these three genes is supported by the high coverage of the involved plastome assemblies, which ranges from 239 to 987× (Table S2). Plastid *ndh* genes, together with a set of nuclear loci, encode a subunit of the plastome NDH (NADH dehydrogenase-like) complex involved in cyclic electron flow (CEF) in photosynthesis (Martín & Sabater, 2010; Strand et al., 2019). In general, significant *ndh* gene losses have been commonly reported for parasitic plants (Ruhlman et al., 2015), mycoheterotrophs (e.g., Orchidaceae; Barrett et al., 2019), and carnivorous plants (Yao et al., 2019), associated to reduction or absence of photosynthetic activity. However, multiple losses have been reported in fully photosynthetic plant lineages such as gymnosperms (e.g., Pinaceae; Strand et al., 2019), aquatic plants (e.g., *Littorella uniflora* (L.) Asch.; Mower et al., 2021), and xerophytic species (e.g., Yao et al., 2019). Previous studies have found that these genes have, in some cases, been translocated to other genome compartments, like the mitochondrial genome in some Orchidaceae lineages (Lin et al., 2015) or the nuclear genome in Saguaro (*Carnegiea gigantea* (Engelm.) Britton & Rose, Cactaceae; Sanderson et al., 2015), although they are probably nonfunctional (Ruhlman et al., 2015; Sanderson et al., 2015). Future studies focused on sequencing nuclear and mitochondrial Hechtioideae genomes could help determine if these three genes have been translocated to other genome compartments, if not completely absent. Besides the transfer of genetic content between different genome compartments, loss of *ndh* genes in photosynthetic groups has been related to light, nutrient, and water requirements (Sanderson et al., 2015; Strand et al., 2019; Könyves et al., 2021; Mower et al., 2021). In Saguaro, a species that presents the same morphological (succulence) and physiological (photosynthesis CAM) traits adapted to dry and semiarid habitats as Hechtioideae species, Sanderson et al. (2015) proposed that the plastid NDH-like complex is unnecessary, as CEF may be assumed by an alternative system, the Antimycin A-sensitive CEF pathway (see Ruhlman et al., 2015), the genes involved in this pathway being more important, such as the nuclear-encoded gene *pgr5*. In *L. uniflora*, a semiaquatic and CAM species, Mower et al. (2021) suggested that CAM modifications facilitated photosynthesis, making the NDH complex less essential for a functional photosynthetic process. Future studies focused on the survey of genes involved in this alternative nuclear-encoded pathway, combined with ecological and biochemical studies, could identify potential routes of *ndh* gene loss in Hechtioideae.

4.2 A phylogenomic framework for resolving relationships within Hechtioideae

Our study using complete plastome data yielded a strongly supported topology that retrieved Hechtioideae and its three genera as monophyletic, consistent with previous phylogenetic studies (Givnish et al., 2011; Ramírez-Morillo et al., 2018a; Rivera-Martínez et al., 2022; Romero-Soler et al., 2022a). Here, *Mesoamerantha* is resolved as sister to a clade formed by *Bakerantha* and *Hechtia*, which is congruent with the findings of Givnish et al. (2011) based on eight plastid markers, although differing from those proposed in previous studies focusing exclusively on the subfamily and using both plastid and nuclear Sanger sequenced markers (Ramírez-Morillo et al., 2018a; Rivera-Martínez et al., 2022). Discordances between plastid and nuclear data have been associated with biological processes such as incomplete lineage sorting and hybridization (Naciri & Linder, 2015), both of which important mechanisms in the evolution of several Bromeliaceae lineages (Palma-Silva et al., 2016), and reported at the genus (e.g., Tillandsioideae; Loiseau et al., 2021) or species level (e.g., *Aechmea* subgenus *Ortgiesia*, Goetze et al., 2017; *Bakerantha*, Romero-Soler et al., 2022b).

Within *Hechtia*, we recovered similar relationships to that found by Ramírez-Morillo et al. (2018a) and Rivera-Martínez et al. (2022), who used a handful of Sanger sequenced loci, albeit with improved statistical support. Here, we found *H. myriantha* as sister of a clade composed of clades D–E and F proposed by Ramírez-Morillo et al. (2018a). These results are in line with analysis based on plastid data (Ramírez-Morillo et al., 2018b), but incongruent with hypotheses based on nuclear and combined nuclear and plastid data (Ramírez-Morillo et al., 2018a; Rivera-Martínez et al., 2022), which recovered *H. myriantha* embedded within clade D, the latter clade formed by species of the *H. glomerata* complex. Clades D–E herein show low statistical support (BS = 52; Fig. 3), likely due to the extremely short subtending internode. An expanded sampling including more species of clade D and *H. epigyna* from clade E could confirm or refute the monophyly of each of these two clades. As in previous phylogenetic studies, clade F is characterized herein by short internodes with low to moderate statistical support. Thus, even with complete plastid genome sequence data, support for relationships at shallower phylogenetic divergences within that clade remains low to moderate, pointing to the need to seek more variable molecular markers such as low-copy nuclear loci, as has been explored recently for other rapidly radiating bromeliad lineages (Loiseau et al., 2021; Yardeni et al., 2022; Bratzel et al., 2023).

4.3 Informative plastid loci in Hechtioideae

Sanger sequenced markers have been the main source of data in the phylogenetic studies in Bromeliaceae (reviewed by Palma-Silva et al., 2016), including Hechtioideae. We assessed the net PI of 209 plastid loci that comprised 93 coding and 116 noncoding (introns and IGS) regions included in our final plastid matrix (Fig. 4; Table S4). The PI of noncoding regions was higher than that of coding genes (Fig. 4), which is a common phenomenon in plants as coding genes tend to be more conserved, while the noncoding regions are prone to higher rates of nucleotide substitution (Clegg et al., 1994; Borsch & Quandt, 2009). This variation in

substitution rates has made noncoding regions the first choice in marker selection in plant systematics due to their potential phylogenetic utility (Borsch & Quandt, 2009; Shaw et al., 2014).

Only a few plastid loci have been used in previous studies focusing strictly on Hechtioideae, including part of the *matK* and *ycf1* genes, and the intergenic spacers *rpl32-trnL* and *trnK-rps16* (Ramírez-Morillo et al., 2018a; Rivera-Martínez et al., 2022; Romero-Soler et al., 2022a, 2022b). Here, our PI analysis yielded the *ycf1* gene as the locus with the highest maximum net PI (Fig. 4; Table S4). This gene is nearly three times more informative than most of the analyzed loci (maximum net PI value = 3.8, Fig. 4), and, although its maximum net PI is at deep divergences, it presents high informativeness toward time 0. The *ycf1* gene has been recently reported as the most informative loci in Tillandsioideae (Vera-Paz et al., 2022), and has been used in Bromeliaceae at different phylogenetics depths (e.g., Barfuss et al., 2016; Castello et al., 2016; Matuszak-Renger et al., 2018; Leme et al., 2021). Furthermore, the high performance of this gene in resolving relationships at different taxonomic scales and phylogenetic depths has been identified in several plant lineages (e.g., Ortiz-Rodríguez et al., 2018; Granados Mendoza et al., 2020) and has even been considered an alternative to previously proposed barcodes (Dong et al., 2015).

Although the *matK* gene and *trnK-rps16* IGS have been widely used in bromeliad phylogenetics (Palma-Silva et al., 2016), they are not among the most informative markers in Hechtioideae, with 16th and 26th positions in terms of ranking, respectively (Table S4). In the case of the *rpl32-trnL* IGS, we exclude it from our PI analysis since it was included in a large inversion in *H. deceptrix*, along with other loci such as *ndhF*, *rpl32, trnL*, and *ccsA* and their intergenic spacers, as they were not homologous across our taxon sampling. However, in previous studies in Hechtioideae, the *rpl32-trnL* IGS presents percentages of phylogenetically informative characters slightly lower than those found in the *ycf1* fragments included (5.8 vs. 6.7%, respectively; Ramírez-Morillo et al., 2018a), and has provided good resolution for intraspecific relationships in less diverse lineages (e.g., *Bakerantha*; Romero-Soler et al., 2022a, 2022b).

Our results suggest that marker selection in Hechtioideae can be improved, since loci used in previous studies reach their maximum net PI toward the root of Bromeliaceae (Fig. 4) and show limited utility for resolving relationships among closely related species, as has been found for the same set of markers in Tillandsioideae (Vera-Paz et al., 2022). When comparing the ten loci with the highest net PI identified in this study with those found in Tillandsioideae (see Vera-Paz et al., 2022), only four common loci were observed (*ycf1* gene, *rpoC2* gene, *rpl16* intron, and *psbE-petL* IGS). The differences in the PI of the loci among bromeliad lineages show the need for taxon-specific markers assessments, as has been recently suggested in the study of Puyoideae by Liu et al. (2022).

Of the ten loci with the highest net PI, none had been explored before for Hechtioideae phylogenetics, except the *ycf1* gene, but a few have been used or proposed as alternatives in other bromeliad lineages such as the *trnS-trnG* IGS (Puyoideae, Jabaily & Sytsma, 2010; Liu et al., 2022),

rps16-trnQ IGS (*T. ionantha* Planch. complex; Ancona et al., 2022), and *rpoB-trnC* IGS (Puyoideae, Liu et al., 2022). Other markers such as the noncoding regions *trnT-psbD* IGS, *ndhC-trnV* IGS, and *atpF* intron, previously recognized for being highly variable across angiosperms lineages (Shaw et al., 2014), could be additional loci suitable for Sanger sequencing in Hechtioideae. Furthermore, the *trnT-psbD* and *trnS-trnG* intergenic spacers, which reach their maximum informativeness at shallow evolutionary depths within *Hechtia*, could be used to solve recalcitrant relationships of recently diverged lineages (e.g., clade F of *Hechtia*) and applied in future phylogeographic studies, since most groups of haplotypes do not require full internal resolution (Gitzendanner et al., 2018).

4.4 Plastome attributes' evolution in Hechtioideae

The phenotypic evolution analysis in BAMM detected eleven shifts in the rates of evolution in four out of the eight analyzed plastome attributes. Four of these shifts were allocated in Bromelioideae and Tillandsioideae clades and were related to SSC and IR sizes and IR GC content attributes. This is consistent with the IR expansion and an associated LSC reduction of the Bromelioideae species *F. bicolor* reported by Paule et al. (2020). In the case of *T. usneoides* (Tillandsioideae), the shift identified is related to its small IR size, one of the smallest reported by Vera-Paz et al. (2022) for Tillandsioideae species.

The seven remaining shifts were detected in *H. deceptrix* and the clade F. In *H. deceptrix*, three shifts were detected associated with SSC and IR sizes and IR GC content. As mentioned above, the detected IR expansion involves the translocation of four genes from the SSC to the IR (*ycf1*, *rps15*, and *ndhH* full genes, and a partial *ndhA* gene), resulting in a large reduction of the SSC region (Fig. 2; Table 1). A similar rearrangement related to the SSC/IR junction is known for other Poales, being characteristic of the grass family (Poaceae; Guisinger et al., 2010), and among other monocot lineages such as in *Strumaria truncata* Jacq. (Amaryllidaceae; Könyves et al., 2021). Additionally, *H. deceptrix* has the lowest IR GC content (40%; Table S3), like that found in the IR of the *Tillandsia* clade K.1, which also underwent an IR expansion (Vera-Paz et al., 2022). When genes are transferred into the IR from a single-copy region, deceleration of substitution rates and increments of GC content can be expected (Li et al., 2016; Yang et al., 2022). Vera-Paz et al. (2022) suggested that in recently diverged lineages, enough time might not have elapsed, and the IR is still in the process of GC content stabilization. This might be the case in *H. deceptrix*, which diverged only about 1.9 Mya from its close relatives (Rivera-Martínez et al., 2022), and the translocated genes into the IR could still be in an early process of substitution rate deceleration consistent with their new position in the plastome (Mower & Vickrey, 2018; Vera-Paz et al., 2022). *Hechtia deceptrix* has undergone several genomic rearrangements compared to other Hechtioideae and bromeliad species. Morphologically, this *Hechtia* species differs from others in the genus in presenting inferior ovaries (vs. superior or ¾ inferior ovaries, except in *H. epigyna*, which also has inferior ovaries), and it is geographically restricted to xerophytic vegetation in a semidesert in the Mexican state of Hidalgo. Further comparative

studies are necessary to assess whether the plastome changes detected in *H. deceptrix* are exclusive of this species or present in other Hechtioideae lineages.

Three shifts were assigned to clade F, including changes in SSC and IR sizes and IR GC content (Fig. 5). These shifts are associated with a small IR contraction at the SSC/IR border that results in the complete transfer of the *ycf1* gene to the SSC region (Figs. 2, S2). A single shift in the SSC GC content was detected in a subclade of clade F, including six species, most of them with a relatively high GC content (>31.57%). Overall, the clade F has undergone several small genome rearrangements, along with important potential pseudogenization and gene loss in the *ndh* gene family (Fig. 3). This clade experienced rapid species diversification in the last 5.7 Mya, associated with several dispersal events and subsequent *in situ* speciation, most events related to the colonization of dry habitats (Rivera-Martínez et al., 2022). Future studies could assess if these plastome reorganizations have played an important role in the diversification of this recently diverged group of Hechtioideae.

5 Conclusions

Genomic structural rearrangements have occurred throughout the evolution of Hechtioideae plastomes, including expansions and contractions of the IR. Also, here, we documented for the first time several cases of possible pseudogenization and loss of the *ndh* gene family in Bromeliaceae. An expanded taxonomic sampling in this lineage can help determine if these structural rearrangements are clade specific or have occurred several times in the Hechtioideae evolution. The phylogenomic plastid analyses demonstrate the utility of a complete plastid genome in resolving relationships between the Hechtioideae genera; however, statistical support for shallower phylogenetic divergences is still limited. Within *Hechtia*, the relationships are in line with those proposed in previous studies using a few loci, and this approach in general allowed to increase node support for some recalcitrant nodes. However, additional nuclear single-copy loci data might be needed to resolve difficult lineages like clade F of *Hechtia*. A promising group of alternative highly informative markers is proposed herein for Sanger sequencing, in addition to the possibility of using the whole-plastid genome as a super-barcode. Evolutionary trait rate shifts were associated with changes in the size and GC content of the SSC and IRs; further studies are needed to assess if these shifts are related to species diversification in this bromeliad subfamily.

Acknowledgements

References

Ancona JJ, Pinzón-Esquivel JP, Ruiz-Sánchez E, Palma-Silva C, Ortiz-Díaz JJ, Tun-Garrido J, Carnevali G, Raigoza NE. 2022. Multilocus data analysis reveal the diversity of cryptic species in the *Tillandsia ionantha* (Bromeliaceae: Tillansioideae) complex. *Plants* 11(13): 1706.

Amiryousefi A, Hyvönen J, Poczai P. 2018. IRscope: An online program to visualize the junction sites of chloroplast genomes. *Bioinformatics* 34(17): 3030–3031.

Andrews S. 2018. FastQC: A quality control tool for high throughput sequence data [online]. Available from https://www.bioinformatics.babraham.ac.uk/projects/fastqc/[accessed 10 November 2022]

Barfuss MHJ, Till W, Leme EM, Pinzón JP, Manzanares JM, Halbritter H, Samuel R, Brown GK. 2016. Taxonomic revision of Bromeliaceae subfam. Tillandsioideae based on a multi-locus DNA sequence phylogeny and morphology. *Phytotaxa* 279: 1–97.

Barrett CF, Sinn BT, Kennedy AH. 2019. Unprecedented parallel photosynthetic losses in a heterotrophic Orchid genus. *Molecular Biology and Evolution* 36(9): 1884–1901.

Bolger AM, Lohse M, Usadel B. 2014. Trimmomatic: A flexible trimmer for Illumina sequence data. *Bioinformatics* 30(15): 2114–2120.

Borsch T, Quandt D. 2009. Mutational dynamics and phylogenetic utility of noncoding chloroplast DNA. *Plant Systematics and Evolution* 282: 169–199.

Bratzel F, Paule J, Leebens-Mack J, Leme EMC, Forzza RC, Koch MA, Heller S, Zizka G. 2023. Target-enrichment sequencing reveals for the first time a well-resolved phylogeny of the core Bromelioideae (family Bromeliaceae). *Taxon* 72(1): 47–63.

Castello LV, Barfuss MH, Till W, Galetto L, Chiapella JO. 2016. Disentangling the *Tillandsia capillaris* complex: Phylogenetic relationships and taxon boundaries in Andean populations. *Botanical Journal of the Linnean Society* 181: 391–414.

Castresana J. 2000. Selection of conserved blocks from multiple alignments for their use in phylogenetic analysis. *Molecular Biology and Evolution* 17: 540–552.

Chan PP, Lowe TM. 2019. tRNAscan-SE: Searching for tRNA genes in genomic sequences. In: Kollmar M ed. *Gene prediction: Methods and protocols*. New York: Springer. 1–14.

Chávez-Galarza JC, Cardenas-Ninasivincha S, Contreras R, Ferro-Mauricio R, Huanca-Mamani W. 2021a. Chloroplast genoma of *Tillandsia marconae* Till & Vitek (Bromeliaceae), a hyperarid desert endangered species. *Mitochondrial DNA Part B* 6(9): 2562–2564.

Chávez-Galarza JC, Cardenas-Ninasivincha S, Contreras R, Ferro-Mauricio R, Huanca-Mamani W. 2021b. Chloroplast genome of

Tillandsia landbeckii Phil. (Bromeliaceae) a species adapted to the hyper-arid conditions of the Atacama and Peruvian desert. *Mitochondrial DNA Part B* 6(12): 3375–3377.

Clegg MT, Gaut BS, Learn GH, Morton BR. 1994. Rates and patterns of chloroplast DNA evolution. *Proceedings of the National Academy of Sciences United States of America* 91: 6795–6801.

Dong W, Xu C, Li C, Sun J, Zuo Y, Shi S, Cheng T, Guo J, Zhou S. 2015. *ycf1*, the most promising plastid DNA barcode of land plants. *Scientific Reports* 5: 8348.

Doyle JJ, Doyle JL. 1987. A rapid DNA isolation procedure for small quantities of fresh leaf tissue. *Phytochemical Bulletin* 19: 11–15.

Faircloth BC, Chang J, Alfaro ME. 2012. TAPIR enables high-throughput estimation and comparison of phylogenetic informativeness using locus-specific substitution models. *arXiv*. Available from https://arxiv.org/abs/1202.1215

Gao L, Su YJ, Wang T. 2010. Plastid genome sequencing, comparative genomics, and phylogenomics: Current status and prospects. *Journal of Systematics and Evolution* 48: 77–93.

Gitzendanner MA, Soltis PS, Yi TS, Li DZ, Soltis DE. 2018. Chapter Ten—Plastome phylogenetics: 30 years of inferences into plant evolution. In: Chaw SM, Jansen RK eds. *Advances in botanical research*. Cambridge: Academic Press. 293–313.

Givnish TJ, Barfuss MH, Van Ee B, Riina R, Schulte K, Horres R, Gonsiska PA, Jabaily RS, Crayn DM, Smith JA. 2011. Phylogeny, adaptive radiation, and historical biogeography in Bromeliaceae: Insights from an eight-locus plastid phylogeny. *American Journal of Botany* 98: 872–895.

Givnish TJ, Millam KC, Berry PE, Sytsma KJ. 2007. Phylogeny, adaptive radiation, and historical biogeography of Bromeliaceae inferred from *ndhF* sequence data. *Aliso* 23: 3–26.

Goetze M, Zanella CM, Palma-Silva C, Büttow MV, Bered F. 2017. Incomplete lineage sorting and hybridization in the evolutionary history of closely related, endemic yellow-flowered *Aechmea* species of subgenus *Ortgiesia* (Bromeliaceae). *American Journal of Botany* 104: 1073–1087.

Gouda EJ, Butcher D, Gouda CS. 2023. *Encyclopaedia of bromeliads, version 5*. Utrecht: University Botanic Gardens. Available from http://bromeliad.nl/encyclopedia [accessed 20 January 2023].

Granados Mendoza C, Jost M, Hágsater E, Magallón S, van den Berg C, Lemmon EM, Lemmon AR, Salazar GA, Wanke S. 2020. Target nuclear and off-target plastid hybrid enrichment data inform a range of evolutionary depths in the orchid genus *Epidendrum*. *Frontiers in Plant Science* 10: 1761.

Guisinger MM, Chumley TW, Kuehl JV, Boore JL, Jansen RK. 2010. Implications of the plastid genome sequence of *Typha* (Typhaceae, Poales) for understanding genome evolution in Poaceae. *Journal of Molecular Evolution* 70: 149–166.

Jabaily RS, Sytsma KJ. 2010. Phylogenetics of *Puya* (Bromeliaceae): Placement, major lineages, and evolution of Chilean species. *American Journal of Botany* 97(2): 337–356.

Jansen RK, Ruhlman TA. 2012. Plastid genomes of seed plants. In: Bock R, Knoop V eds. *Genomics of chloroplasts and mitochondria*. Dordrecht: Springer. 103–126.

Jin JJ, Yu WB, Yang JB, Song Y, Depamphilis CW, Yi TS, Li DZ. 2020. GetOrganelle: A fast and versatile toolkit for accurate de novo assembly of organelle genomes. *Genome Biology* 21: 241.

Katoh K, Standley DM. 2013. MAFFT Multiple Sequence Alignment Software Version 7: Improvements in performance and usability. *Molecular Biology and Evolution* 30: 772–780.

Kearse M, Moir R, Wilson A, Stones-Havas S, Cheung M, Sturrock S, Buxton S, Cooper A, Markowitz S, Duran C. 2012. Geneious basic: An integrated and extendable desktop software platform for the organization and analysis of sequence data. *Bioinformatics* 28: 1647–1649.

Könyves K, Bilsborrow J, Christodoulou MD, Culham A, David J. 2021. Comparative plastomics of Amaryllidaceae: Inverted repeat expansion and the degradation of the *ndh* genes in *Strumaria truncata* Jacq. *PeerJ* 9: e12400.

Leme EMC, Zizka G, Paule J, Aguirre-Santoro J, Heller S, Ramírez-Morillo IM, Halbritter H, Mariath JEA, Carvalho JDT, Forzza RC. 2021. Re-evaluation of the Amazonian *Hylaeaicum* (Bromeliaceae: Bromelioideae) based on neglected morphological traits and molecular evidence. *Phytotaxa* 499: 1–60.

Li F-W, Kuo L-Y, Pryer KM, Rothfels CJ. 2016. Genes translocated into the plastid inverted repeat show decelerated substitution rates and elevated GC content. *Genome Biology and Evolution* 8(8): 2452–2458.

Li H, Durbin R. 2009. Fast and accurate short read alignment with Burrows-Wheeler Transform. *Bioinformatics* 25: 1754–1760.

Li H, Handsaker B, Wysoker A, Fennell T, Ruan J, Homer N, Marth G, Abecasis G, Durbin R. 2009. The sequence Alignment/Map format and SAMtools. *Bioinformatics* 25(16): 2078–2079.

Lin CS, Chen J, Huang YT, Chan M-T, Daniell H, Chang WJ, Hsu C-T, Liao DC, Wu F-H, Lin S-Y, Liao C-F, Deyholos MK, Wong G K-S, Albert VA, Chou M-L, Chen C-Y, Shih MC. 2015. The location and translocation of ndh genes of chloroplast origin in the Orchidaceae family. *Scientific Reports* 5: 9040.

Liu L, Zhang YQ, Tumi L, Suni ML, Arakaki M, Burgess KS, Ge XJ. 2022. Genetic markers in Andean *Puya* species (Bromeliaceae) with implications on plastome evolution and phylogeny. *Ecology and Evolution* 12(8): e9159.

Lohse M, Drechsel O, Kahlau S, Bock R. 2013. OrganellarGenomeDRAW—A suite of tools for generating physical maps of plastid and mitochondrial genomes and visualizing expression data sets. *Nucleic Acids Research* 41: 575–581.

Loiseau O, Mota Machado T, Paris M, Koubínová D, Dexter KG, Versieux LM, Lexer C, Salamin N. 2021. Genome skimming reveals widespread hybridization in a Neotropical flowering plant radiation. *Frontiers in Ecology and Evolution* 9: 668281.

Lowe TM, Chan PP. 2016. tRNAscan-SE on-line: Integrating search and context for analysis of transfer RNA genes. *Nucleic Acids Research* 44: W54–W57.

Machado TM, Loiseau O, Paris M, Weigand A, Versieux LM, Stehmann JR, Lexer C, Salamin N. 2020. Systematics of *Vriesea* (Bromeliaceae): Phylogenetic relationships based on nuclear gene and partial plastome sequences. *Botanical Journal of the Linnean Society* 192: 656–674.

Martín M, Sabater B. 2010. Plastid *ndh* genes in plant evolution. *Plant Physiology and Biochemistry* 48: 636–645.

Matuszak-Renger S, Paule J, Heller S, Leme EMC, Steinbeisser GM, Barfuss MHJ, Zizka G. 2018. Phylogenetic relationships among *Ananas* and related taxa (Bromelioideae, Bromeliaceae) based on nuclear, plastid and AFLP data. *Plant Systematics and Evolution* 304: 841–851.

Miller MA, Pfeiffer W, Schwartz T. 2010. Creating the CIPRES Science Gateway for inference of large phylogenetic trees. In: *Proceedings of the Gateway Computing Environments Workshop (GCE)*. New Orleans: IEEE. 1–8.

Milne I, Stephen G, Bayer M, Cock PJA, Pritchard L, Cardle L, Shaw PD, Marshall D. 2013. Using Tablet for visual exploration of second-generation sequencing data. *Briefings in Bioinformatics* 14(2): 193–202.

Möbus J, Kiefer C, Quandt D, Barfuss MH, Koch MA. 2021. Setting the evolutionary timeline: *Tillandsia landbeckii* in the Chilean Atacama Desert. *Plant Systematics and Evolution* 307: 39.

Mower JP, Vickrey TL. 2018. Chapter Nine—Structural diversity among plastid genomes of land plants. In: Chaw SM, Jansen RK eds. *Advances in botanical research*. Cambridge: Academic Press. 263–292.

Mower JP, Guo W, Partha R, Fan W, Levsen N, Wolff K, Nugent JM, Pabon-Mora N, Gonzalez F. 2021. Plastomes from tribe Plantagineae (Plantaginaceae) reveal infrageneric structural synapormorphies and localized hypermutation for Plantago and functional loss of ndh genes from Littorella. *Molecular Phylogenetics and Evolution* 162: 107217.

Naciri Y, Linder HP. 2015. Species delimitation and relationships: The dance of the seven veils. *Taxon* 64: 3–16.

Nashima K, Terakami S, Nishitani C, Kunihisa M, Shoda M, Takeuchi M, Urasaki N, Tarora K, Yamamoto T, Katayama H. 2015. Complete chloroplast genome sequence of pineapple (*Ananas comosus*). *Tree Genetics and Genomes* 11: 60.

Ortiz-Rodríguez AE, Ornelas JF, Ruiz-Sanchez E. 2018. A jungle tale: Molecular phylogeny and divergence time estimates of the *Desmopsis-Stenanona* clade (Annonaceae) in Mesoamerica. *Molecular Phylogenetics and Evolution* 122: 80–94.

Palma-Silva C, Leal BSS, Chaves CJN, Fay MF. 2016. Advances in and perspectives on evolution in Bromeliaceae. *Botanical Journal of the Linnean Society* 181: 305–322.

Palmer JD. 1983. Chloroplast DNA exists in two orientations. *Nature* 301: 92–93.

Palmer JD. 1991. Plastid chromosomes: Structure and evolution. In: Bogorad L, Vasil IK eds. *The molecular biology of plastids*. Cambridge: Academic Press. 5–53.

Paradis E, Schliep K. 2019. ape 5.0: An environment for modern phylogenetics and evolutionary analyses in R. *Bioinformatics* 35: 526–528.

Paule J, Schmickl R, Fér T, Matuszak-Renger S, Halbritter H, Zizka G. 2020. Phylogenomic insights into the *Fascicularia-Ochagavia* group (Bromelioideae, Bromeliaceae). *Botanical Journal of the Linnean Society* 192(4): 642–655.

Plummer M, Best N, Cowles K, Vines K. 2006. CODA: Convergence diagnosis and output analysis for MCMC. *R News* 6: 7–11.

Poczai P, Hyvönen J. 2017. The complete chloroplast genome sequence of the CAM epiphyte Spanish moss (*Tillandsia usneoides*, Bromeliaceae) and its comparative analysis. *PLoS One* 12: 1–25.

Pond SLK, Frost SDW, Muse SV. 2005. HyPhy: Hypothesis testing using phylogenies. *Bioinformatics* 21: 676–679.

R Core Team. 2022. *R: A language and environment for statistical computing*. Vienna: R Foundation for Statistical Computing.

Rabosky DL. 2014. Automatic detection of key innovations, rate shifts, and diversity-dependence on phylogenetic trees. *PLoS One* 9: e89543.

Ramírez-Morillo IM, Carnevali G, Pinzón JP, Romero-Soler K, Raigoza N, Hornung-Leoni N, Duno R, Tapia-Muñoz JL, Echevarría I. 2018a. Phylogenetic relationships of *Hechtia* (Hechtioideae; Bromeliaceae). *Phytotaxa* 376: 227–253.

Ramírez-Morillo IM, Romero-Soler K, Carnevali G, Pinzón JP, Raigoza N, Hornung-Leoni C, Duno R, Tapia-Muñoz JL. 2018b. The reestablishment of *Bakerantha*, and a new genus in Hechtioideae (Bromeliaceae) in Megamexico, *Mesoamerantha*. *Harvard Papers in Botany* 23: 301–312.

Redwan RM, Saidin A, Kumar SV. 2015. Complete chloroplast genome sequence of MD-2 pineapple and its comparative analysis among nine other plants from the subclass Commelinidae. *BMC Plant Biology* 15: 196.

Revell LJ. 2012. phytools: An R package for phylogenetic comparative biology (and other things). *Methods in Ecology and Evolution* 3: 217–223.

Rivera-Martínez R, Ramírez-Morillo IM, De-Nova JA, Carnevali G, Pinzón JP, Romero-Soler KJ, Raigoza N. 2022. Spatial phylogenetics in Hechtioideae (Bromeliaceae) reveals a recent speciation and dispersal. *Botanical Science* 100(3): 692–709.

Romero-Soler KJ, Ramírez-Morillo IM, Ruiz-Sánchez E, Hornung-Leoni C, Carnevali G, Raigoza N. 2022a. Phylogenetic relationships within the Mexican genus *Bakerantha* (Hechtioideae, Bromeliaceae) based on plastid and nuclear DNA: Implications for taxonomy. *Journal of Systematics and Evolution* 60: 55–72.

Romero-Soler KJ, Ramírez-Morillo IM, Ruiz-Sánchez E, Hornung-Leoni C, Carnevali G. 2022b. Historical biogeography and comparative phylogeography of the Mexican bromeliad genus *Bakerantha*: Insights into evolution and diversification. *Botanical Journal of the Linnean Society* 199(1): 109–127.

Ruhlman TA, Chang WJ, Chen JJW, Huang YT, Chan MT, Zhang J, Liao DC, Blazier JC, Jin X, Shih MC, Jansen RK, Lin CS. 2015. NDH expression marks major transitions in plant evolution and reveals coordinate intracellular gene loss. *BMC Plant Biology* 15: 100.

Sanderson MJ, Copetti D, Burquez A, Bustamante E, Charboneau JL, Eguiarte LE, Kumar S, Lee HO, Lee J, McMahon M, Steele K, Wing R, Yang T-J, Zwickl D, Wojciechowski MF. 2015. Exceptional reduction of the plastid genome of saguaro cactus (*Carnegiea gigantea*): Loss of the ndh gene suite and inverted repeat. *American Journal of Botany* 102: 1115–1127.

Sass C, Specht CD. 2010. Phylogenetic estimation of the core Bromelioids with emphasis on the genus *Aechmea* (Bromeliaceae). *Molecular Phylogenetics and Evolution* 55: 559–571.

Shaw J, Shafer HL, Leonard OR, Kovach MJ, Schorr M, Morris AB. 2014. Chloroplast DNA sequence utility for the lowest phylogenetic and phylogeographic inferences in angiosperms: The tortoise and the hare IV. *American Journal of Botany* 101(11): 1987–2004.

Smith SA, Donoghue MJ. 2008. Rates of molecular evolution are linked to life history in flowering plants. *Science* 322: 86–89.

Stamatakis A. 2014. RAxML Version 8: A tool for phylogenetic analysis and post–analysis of large phylogenies. *Bioinformatics* 30: 1312–1313.

Strand DD, D'Andrea L, Bock R. 2019. The plastid NAD(P)H dehydrogenase-like complex: Structure, function and evolutionary dynamics. *Biochemical Journal* 476: 2743–2756.

Townsend JP. 2007. Profiling phylogenetic informativeness. *Systematic Biology* 56: 222–231.

Vera-Paz SI, Díaz Contreras Díaz DD, Jost M, Wanke S, Rossado AJ, Hernández-Gutiérrez R, Salazar GA, Magallón S, Gouda EJ, Ramírez-Morillo IM, Donadío S, Granados Mendoza C. 2022. New plastome structural rearrangements discovered in core Tillandsioideae (Bromeliaceae) support recently adopted taxonomy. *Frontiers in Plant Science* 13: 924922.

Vera-Paz SI, Granados Mendoza C, Díaz Contreras Díaz DD, Jost M, Salazar GA, Rossado AJ, Montes-Azcué CA, Hernández-Gutiérrez R, Magallón S, Sánchez-González LA, Gouda EJ, Cabrera LI, Ramírez-Morillo IM, Flores-Cruz M, Granados-Aguilar X, Martínez-García AL, Hornung-Leoni CT, Barfuss MHJ, Wanke S. 2023. Plastome phylogenomics reveals an early Pliocene North- and Central America colonization by long-distance dispersal from

J. Syst. Evol. 00 (0): 1–17, 2023

www.jse.ac.cn

South America of a highly diverse bromeliad lineage. *Frontiers in Plant Science* 14: 1205511.

Wang RJ, Cheng CL, Chang CC, Wu CL, Su TM, Chaw SM. 2008. Dynamics and evolution of the inverted repeat-large single copy junctions in the chloroplast genomes of monocots. *BMC Evolutionary Biology* 8: 36.

Yang T, Kumar Sahu S, Yang L, Liu Y, Mu W, Liu X, Lenz Strube M, Liu H, Zhong B. 2022. Comparative analyses of 3,654 plastid genomes unravel insights into evolutionary dynamics and phylogenetic discordance of green plants. *Frontiers in Plant Science* 13: 808156.

Yao G, Jin JJ, Li HT, Yang JB, Mandala VS, Croley M, Mostow R, Douglas NA, Chase MW, Christenhusz MJM, Soltis DE, Soltis PS, Smith SA, Brockington SF, Moore MJ, Yi TS, Li DZ. 2019. Plastid phylogenomic insights into the evolution of Caryophyllales. *Molecular Phylogenetics and Evolution* 134: 74–86.

Yardeni G, Viruel J, Paris M, Hess J, Groot Crego C, de La Harpe M, Rivera N, Barfuss MHJ, Till W, Guzmán-Jacob V, Krömer T, Lexer C, Paun O, Leroy T. 2022. Taxon-specific or universal? Using target capture to study the evolutionary history of rapid radiations. *Molecular Ecology Resources* 22: 927–945.

Zhu A, Guo W, Gupta S, Fan W, Mower JP. 2016. Evolutionary dynamics of the plastid inverted repeat: The effects of expansion, contraction, and loss on substitution rates. *New Phytologist* 209: 1747–1756.

Supplementary Material

The following supplementary material is available online for this article at http://onlinelibrary.wiley.com/doi/10.1111/jse.13004/suppinfo:

Fig. S1. Gene map of the plastome of all species newly sequenced in this study. The color depicted in the genes represents their functional category. The innermost gray circle denotes the guanine–cytosine content across the genome. Genes that are transcribed counter-clockwise and clockwise are shown to the outside and the inside of the outer circle, respectively. Genes with introns are marked with an asterisk.

Fig. S2. Comparison of the large single copy (LSC), small single copy (SSC), and inverted repeat (IR) borders of all species used in this study. Genes shown above and below the lines are transcribed clockwise and counter-clockwise, respectively.

Fig. S3. Maximum likelihood tree based on the analysis of 26 complete bromeliad plastomes. Values in branches indicate the node bootstrap support.

Table S1. Taxon sampling, voucher information, and GenBank accession numbers.

Table S2. Information of the *de novo* plastome assemblies of 21 bromeliad species. Number of raw reads (total number of reads product of the sequencing strategy); number of raw reads after quality trimming (total number of reads after removal of adaptors and low-quality sequences); number of mapped reads (total number of trimmed reads that support each plastome sequence); average coverage (*x*, average base coverage of the final plastome assemblies).

Table S3. Plastome attributes of Hechtioideae and other bromeliads species used in this study. Sequences with * were downloaded from NCBI.

Table S4. A, Maximum net phylogenetic informativeness for each analyzed locus. Loci were sorted from high to low maximum net Phylogenetic Informativeness. Loci in bold have been used in previous phylogenetic studies in Hechtioideae. B, Raw phylogenetic informativeness profile data for each analyzed partition.

Table S5. Reconstructed ancestral state node values, including their variance, lower, and upper 95% confidence interval for the studied plastome attributes.

Supplementary information S1. A, Alignment of the complete plastomes of the 26 species used in this study. B, Final reduced alignment used in the phylogenetic analysis, excluding one inverted repeat, inversions (<200 pb), and poorly aligned and divergent regions.